Article DOI: https://doi.org/10.37284/eajenr.5.1.600

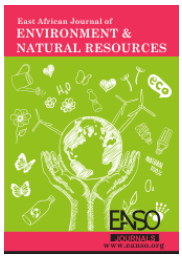

East African Journal of Environment and Natural Resources
eajenr.eanso.org
Volume 5, Issue 1, 2022
Print ISSN: 2707-4234 | Online ISSN: 2707-4242
Title DOI: https://doi.org/10.37284/2707-4242

EAST AFRICAN NATURE & SCIENCE ORGANIZATION

Original Article

Landslide susceptibility mapping using weights of evidence model on the slopes of Mount Elgon, eastern Uganda.

Manasseh Mande[1*], *Denis Nseka*[1] & *Frank Mugagga*[1]

[1] Makerere University, P. O. Box 7062, Kampala, Uganda.
* Correspondence ORCID ID: https://orcid.org/0000-0003-0043-6085; email: mmande23@gmail.com.

Article DOI: https://doi.org/10.37284/eajenr.5.1.600

Date Published:

30 March 2022

Keywords:

Landslides, Susceptibility, Weights of Evidence, Mount Elgon, GIS.

ABSTRACT

Generally, landslide susceptibility mapping is an important step in mitigating their impacts. There is, however, particular dearth of information on the application of GIS-based bivariate methods particularly the weights of evidence model in mapping landslide susceptibility on the slopes of Mount Elgon in eastern Uganda. This study, therefore, evaluated the susceptibility of Bukalasi milli-watershed to landslides, as an early warning strategy for the major landslide hotspot in Uganda. A landslide inventory for the study area was prepared, and the weights of influence of selected landslide-conditioning factors were calculated to present their relative importance in landslide susceptibility. Eight conditioning factors were considered in this study namely; land use, lithology, rainfall, elevation, slope aspect, slope angle, plan curvature and profile curvature. Following the results of the Agterberg-Cheng conditional independence test (probability = 62.5%), the hypothesis of conditional independence among these factors was accepted. Validation using the ROC indicated satisfactory performance of the model considering the model prediction rate (Area under the Curve = 0.882) and success rate (Area under the Curve = 0.912). The final landslide susceptibility map highlights high susceptibility in the southern and western parts of the study area. It further shows that whereas Bukibumbi, Bundesi and Suume parishes are the most prone parishes, Shibanga Parish is relatively the least prone to landslides disasters. Thus, such highly susceptible areas should be prioritised during intervention programmes, especially relocation of the residents at risk. Since the absence of forests has been indicated to exacerbate susceptibility to landslides, deforestation should have severe penalties, and extensive tree-planting should instead be encouraged. Other human activities like farming on fragile slopes, which would further destabilise the slopes should particularly be discouraged.

Article DOI: https://doi.org/10.37284/eajenr.5.1.600

APA CITATION

Mande, M., Nseka, D. & Mugagga, F. (2022). Landslide susceptibility mapping using weights of evidence model on the slopes of Mount Elgon, eastern Uganda. *East African Journal of Environment and Natural Resources*, *5*(1), 97-114. https://doi.org/10.37284/eajenr.5.1.600.

CHICAGO CITATION

Mande, Manasseh, Denis Nseka & Frank Mugagga. 2022. "Landslide susceptibility mapping using weights of evidence model on the slopes of Mount Elgon, eastern Uganda". *East African Journal of Environment and Natural Resources* 5 (1), 97-114. https://doi.org/10.37284/eajenr.5.1.600.

HARVARD CITATION

Mande, M., Nseka, D. & Mugagga, F. (2022) "Landslide susceptibility mapping using weights of evidence model on the slopes of Mount Elgon, eastern Uganda", *East African Journal of Environment and Natural Resources*, 5(1), pp. 97-114. doi: 10.37284/eajenr.5.1.600.

IEEE CITATION

M. Mande, D. Nseka & F. Mugagga, "Landslide susceptibility mapping using weights of evidence model on the slopes of Mount Elgon, eastern Uganda", *EAJENR*, vol. 5, no. 1, pp. 97-114, Mar 2022.

MLA CITATION

Mande, Manasseh, Denis Nseka & Frank Mugagga. "Landslide susceptibility mapping using weights of evidence model on the slopes of Mount Elgon, eastern Uganda". *East African Journal of Environment and Natural Resources*, Vol. 5, no. 1, Mar 2022, pp. 97-114, doi:10.37284/eajenr.5.1.600.

INTRODUCTION

Landslide disasters are some of the effects of climate change (Neema *et al.*,2018) attributed directly or indirectly to human activities (IPCC, 2014; Xing *et al., 2021*). Globally, a total of 4,862 landslide occurrences were recorded between 2004 and 2016 (Froude & Petley, 2018). Uganda, in particular, has recently suffered many losses in several mountainous regions due to landslides. The most devastating landslide disaster in Uganda so far remains the Bududa landslide of March 1, 2010, which destroyed socio-economic infrastructure and killed over 365 people, while displacing several hundreds of people (Kitutu, 2010; Mugagga *et al., 2012*). The frequency of landslides in the area significantly increased from the early 2000s (Nakileza & Nedala, 2020). Uganda's Vision 2040, and the Third National Development Plan (NDPIII) has, therefore, identified the need to strengthen the monitoring and early warning systems for disasters caused by natural hazards including landslides (National Planning Authority, 2020). This would reduce losses, increase resilience, and reduce income inequality among the population. Such important tools include landslide susceptibility maps (Byou, 2021; Xing *et al., 2021*), which show the likelihood of a landslide occurrence in an area on the basis of local inducing factors (Li *et al., 2021*; Pham *et al., 2015*).

Although a significant number of landslide studies have been undertaken on the slopes on Mount Elgon in Eastern Uganda (e.g., Gorokhovich *et al., 2013*; Kitutu, 2010; Kitutu *et al., 2009*; Mugagga *et al., 2012*; Nakileza & Nedala, 2020; Neema *et al., 2018*; Staudt *et al., 2014* etc.), most of them have focused on the conditioning factors, socio-economic implications, risk reduction, landscape evolution and landslide inventories in the region. However, there is specific dearth of information on the application of GIS-based bivariate methods, particularly the weight of evidence model in mapping landslide susceptibility in landslide hotspots such as the Bukalasi milli-watershed. Accordingly, this study, therefore, evaluated the susceptibility of Bukalasi milli-watershed to landslides using weights of evidence model. The study was aimed at determining the extent to which selected landslide-conditioning factors contribute to landslides, thus presenting their relative importance in landslide susceptibility. The evaluation is key for an early warning strategy during the development of resilience plans and community-driven risk-reduction interventions. The calculated weights of influence for selected conditioning factors provide knowledge on the possibilities of managing certain factors in order to reduce the occurrence of landslide disasters. The landslide susceptibility map (LSM) generated for the study area could be used as an essential tool for planners and engineers in sustainable development.

Article DOI: https://doi.org/10.37284/eajenr.5.1.600

METHODS AND MATERIALS

Study area

This study was undertaken in Bukalasi milli-watershed, a landslide hotspot located within Manafwa watershed on the slopes of Mount Elgon, Eastern Uganda (*Figure 1*). The watershed is bound by latitude 0° 59' 17.66" & 1° 3' 2.88", and longitude 34° 23' 24.08" & 34° 26' 24.01". The study area is dominantly hilly, thereby making it more prone to landslide disasters (Kitutu, 2010). The area receives a bimodal rainfall pattern with an average annual amount of 1800 mm (Staudt *et al., 2014*). The wettest periods occur from March to November, while the dry season is mainly from December to March. The mean monthly maximum temperatures range between 25 °C and 29 °C. The soils in the area are described as being mainly Vertisols, characterised by clay content exceeding 41%, therefore, making the area more prone to landslides (Mugagga *et al., 2011*). The slopes consist of material from agglomerates, lavas, nephelinites and phonolites (Staudt *et al., 2014*). Most households in the area are engaged mainly in agriculture with emphasis on food crops such as bananas, cassava, sweet potatoes, yams, beans, maize, and ground nuts. Consequently, much of the land including steep slopes, ranging between 36^{o} and 58^{o} has been cultivated (Mugagga *et al., 2012*), which further increases the risk of landslide occurrences.

Figure 1: Map of study area. Past landslides indicated.

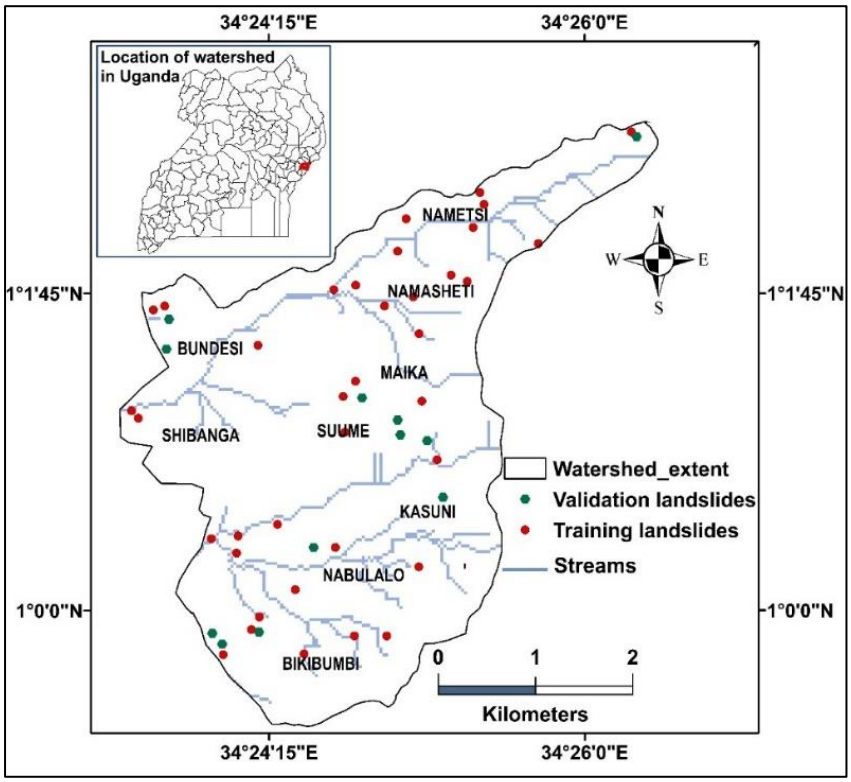

Data Collection

Landslide Inventory Map

The first step in this study was to prepare the landslide inventory map, which specified the locations of the landslides that have occurred in the milli-watershed. Data for the landslide inventory map was obtained from field surveys using Global Positioning System (GPS) mapper and interpretation of aerial photographs as recommended in similar studies (e.g Nohani *et al.*, 2019), particularly Google Earth images taken between 2003 and 2020. Literature search, government reports, community consultations and news reports informed the approximate timelines that aided these interpretations. Presence of debris and removal of vegetation was used as indicators of landslides (*Figure 2*), which was done by comparing images taken before and after landslides processes.

Article DOI: https://doi.org/10.37284/eajenr.5.1.600

Figure 2: Landslide scar observed from Google Earth. Removal of vegetation as an indicator

Field surveys were undertaken to verify the landslide locations identified from Google Earth images. This involved visiting the study area to identify landslide locations, and taking coordinates at the main scarp *(Figure 3)* using GPS mapper using GPS mapper as described by Broeckx et al., (2018). The reliability of the inventory data was enhanced by information from local community members who had witnessed past landslides that were not discernible at the time of the field surveys. Coordinates of the landslide scars were used to build a landslide inventory map of the study area in ArcGIS 10.7 software. This was done by adding the Ms-Excel file (.csv) containing the landslide coordinates into the map of the study area through the 'Add XY Data' icon in the File tool bar of ArcGIS 10.7. The identified landslide locations were then divided into two categories; 75% as the model training datasets and 25% as the test dataset for model validation. This proportion has been proven to give accurate results with limited landslide inventory data (Gadtaula & Dhakal, 2019; Devkota *et al.,* 2013; *Eeckhaut et al.,* 2012). In order to avoid bias, a simple random sampling technique was thus used to group the landslide locations into the two datasets as indicated above.

Figure 3: The main scarp of a landslide in Maika Parish. Photo taken by Mande, November 2020

Article DOI: https://doi.org/10.37284/eajenr.5.1.600

Preparation of Database for the Landslide-Conditioning Factors

Following other landslide susceptibility studies (Benchelha *et al.,* 2019; Broeckx *et al., 2018*; Canavesi *et al., 2020*; Devkota *et al., 2013*; Elmoulat & Lahcen, 2018; Nohani *et al., 2019*), the parameters considered in this study were: topographical parameters (slope angle, slope aspect, elevation, and curvature), lithology, land use and rainfall.

Topographical parameters*:* A 30m Digital Elevation Model (DEM) was downloaded from ASTER global DEM for topographic parameterisation. Voids in the DEM were filled and the watershed was delineated in ArcGIS 10.7. The topographic surfaces including slope angle, elevation, slope aspect, profile curvature and plan curvature were generated, and re-classified to produce the respective maps *(Figures 4 to 8).* These were calculated from the surface option of spatial analyst tools. The output curvature also included plan and profile curvatures, which were the two measures of curvature considered in this study. These topographic parameters were prioritized in this study following several previous studies which reported their importance in landslide susceptibility mapping (Chen *et al., 2019*; Devkota *et al., 2013*; Yalcin *et al., 2011*).

Lithology: The lithology map layer was derived in ArcGIS 10.7, by clipping out the study area from the lithological map obtained from the Directorate of Geological Survey and Mines for Uganda. Lithology was considered important factor in landslide distribution due to its influence soil formation. Differences in soil formation leads to a variation in the soil structure, composition, and permeability, and consequently material strength (Nohani *et al., 2019*). The resulting lithology map of the study area was then classified following the three distinct classes namely: biotite granite, agglomerate, and metagreywacke (*Table 1*; *Figure 9*).

Table 1: Lithological units of study area

Code	Lithology name	Era
NeEag	Volcanic mudflow (lahar), agglomerate, lava	Cenozoic
A3Tbg	Biotite granite	Neoarchaean
A3WBgw	Metagreywacke	Neoarchaean

Land use: The land use distribution for the study area was obtained from the interpretation of 20m sentinel 2A images taken between January 30 and February 06, 2019. The image was freely downloaded from earth explorer (https://earthexplorer.usgs.gov/). The imagery data was imported into ArcGIS 10.7, and a single raster was created from the multiple image bands using the 'Composite Bands' tool in data management. The study area was then clipped from the resulting raster. Using the image classification tool, the training dataset was created by drawing polygons around corresponding land uses on the image classification layer. The training samples were then used in identifying the different land use types following the interactive supervised classification. The major land use types identified were cultivated areas, built-up areas, tropical forests, bare lands, and woodlands *(Figure 10*). The use of such images was cost-effective, and was also suitable for mountainous or inaccessible areas as recommended by previous studies (Guzzetti *et al., 2012*).

Rainfall: Rainfall data for the study area was obtained from the Uganda National Meteorological Authority (UNMA). A CSV (comma delimited) Excel file was created for the averages of the yearly total rainfall between 2005 and 2019 together with the corresponding coordinates. This file was then added into ArcGIS 10.7 using the Add XY Data tool. Afterward, an interpolation using Inverse Distance Weighting (IDW) was run for these points, and the rainfall map for the study area was extracted by mask. The resulting rainfall map was classified into three main classes by manually setting the intervals (*Figure 11*).

Article DOI: https://doi.org/10.37284/eajenr.5.1.600

Figure 4: Slope angle map of the study area

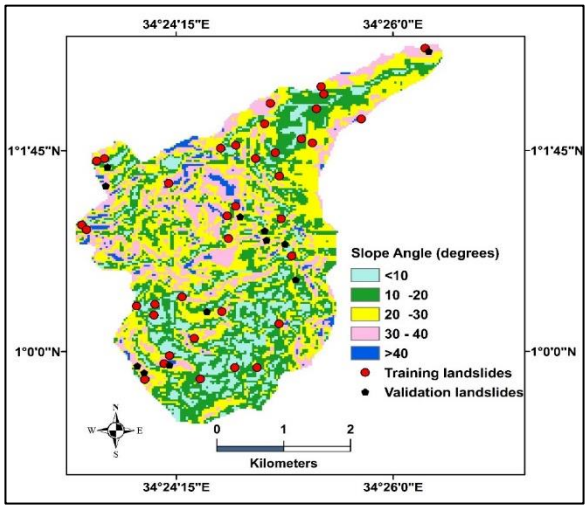

Figure 5: Elevation map of the study area

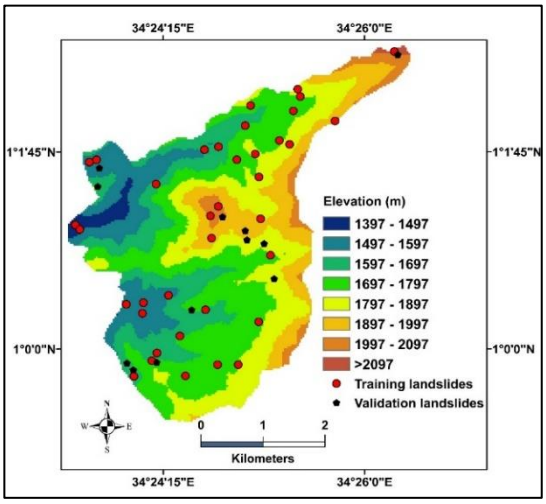

Figure 6: Slope aspect map of study area

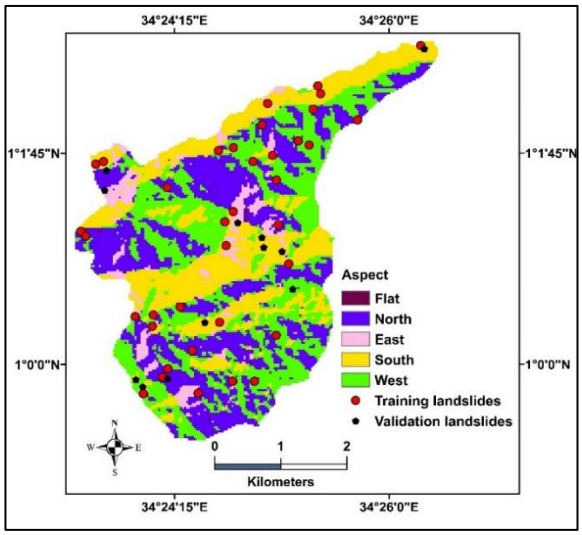

Figure 7: Profile curvature of study area

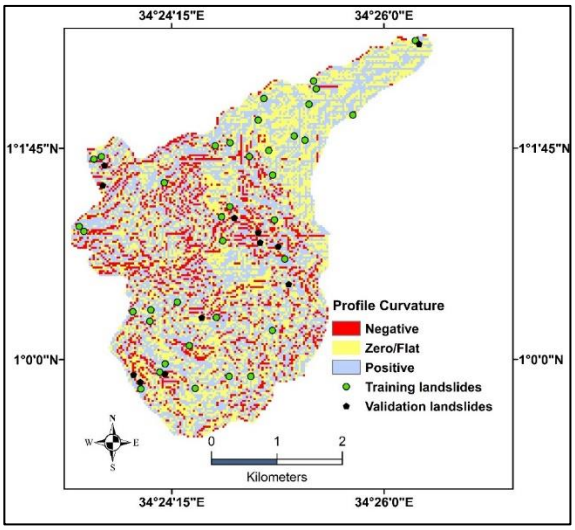

Figure 8: Plan curvature map of study area

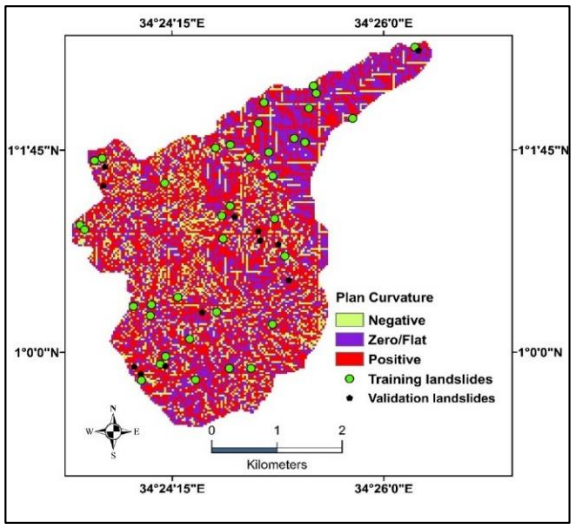

Figure 9: Lithology map of study area

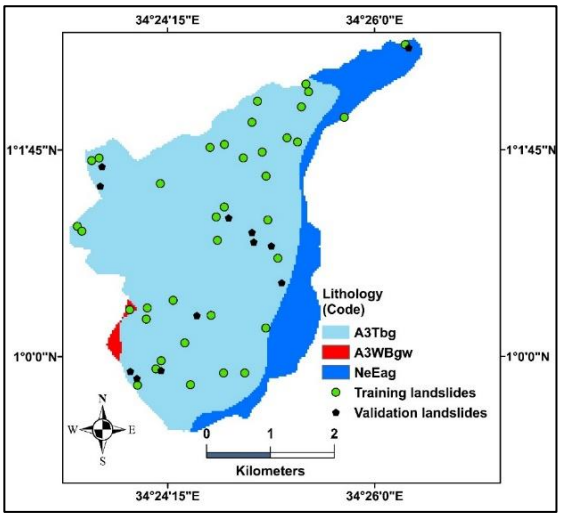

Article DOI: https://doi.org/10.37284/eajenr.5.1.600

Figure 10: Land use map of the study area

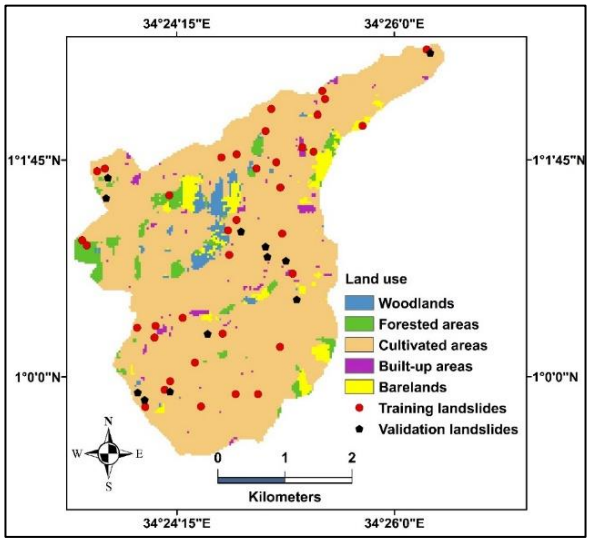

Figure 11: Rainfall map of the study area

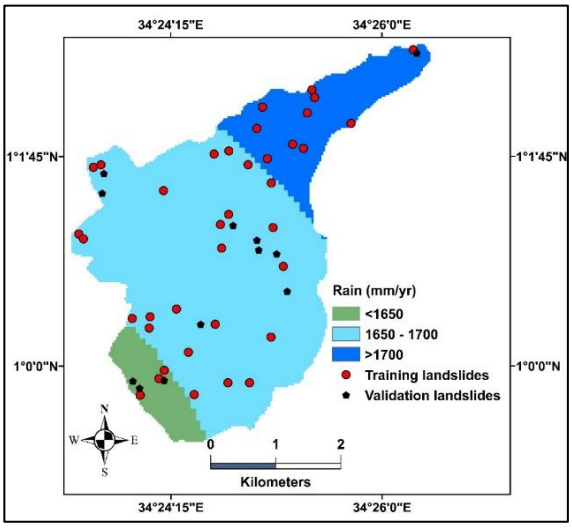

Data Analysis

Application of the Weight of Evidence Model

Every landslide conditioning factor map was crossed with the landslide inventory map using the ArcGIS 10.7 software, and landslide density in each class was calculated, to get the weights for each thematic map (Chen & Li, 2014). The weights of landslide conditioning factors were calculated using the following equations:

$$W+ = \ln\left(\frac{landlside\ area\ in\ considered\ class}{Total\ landslide\ area} \div \frac{stable\ area\ in\ considered\ class}{total\ stable\ area}\right)$$

$$W- = \ln\left(\frac{landlside\ area\ in\ other\ classes}{Total\ landslide\ area} \div \frac{stable\ area\ in\ other\ classes}{total\ stable\ area}\right)$$

The amount of contrast of weights, ($C=W^+ - W^-$), displays the spatial relationship between the landslide conditioning factors (Nohani *et al., 2019*).

The standard deviation of the weights, S(C), was calculated as:

$$S(C) = \sqrt{S^2W^+ + S^2W^-}$$

Where S^2W+, and S^2W- are the variance of positive weights and negative weights, respectively.

The final weight of the landslide conditioning factors and its confidence was obtained by calculating the ratio of the contrast, C, to the standardised contrast, S(C) (Chen & Li, 2014).

The Weight of Evidence was computed using the ArcSDM (Spatial Data Modeller) Tools in ArcGIS 10.7. The weights obtained were then analysed using the calculate response of ArcSDM Tools in ArcGIS 10.7 software, to obtain the final landslide susceptibility map. The susceptibility map was reclassified into five classes namely: very low, low, moderate, high, and very high (Chen *et al., 2019*).

Test for Conditional Independence

The Agterberg-Cheng Conditional Independence (CI) test was applied, since the model assumes conditional independence of the evidence with regards to the training dataset. Agterberg and Cheng (2002), proposed that conditional independence of all the map layers implies that the sum of the posterior probabilities (T) is equal to the total number of discrete events (n). Agterberg-Cheng CI probability values greater than 95% indicates that the hypothesis of conditional independence should be rejected (Elmoulat & Lahcen, 2018). In addition, any value greater than 50% indicates some level of conditional dependence. The test was implemented in the ArcSDM Tools extension of ArcGIS 10.7.

Article DOI: https://doi.org/10.37284/eajenr.5.1.600

Validation of the Model

Twenty-five percent (25%) of the total landslides were used to validate the model using the Receiver Operating Characteristic (ROC), and the Area Under the Curve (AUC) method. Each threshold considered for calculations forms four types of pixels – a binary confusion matrix: the true positive (TP), the false positive (FP), the true negative (TN) and the false negative (FN) (Maxwell *et al., 2021*). The TP and FN pixels are landslides within the classes above and below the threshold, respectively. The TN AND FP pixels are the stable pixels within the classes below and above the value of the threshold, respectively (Vakhshoori & Zare, 2018). Based on the number of pixels for each threshold, two statistics were calculated:

TP rate = FNTP + FN

FP rate = FPTN + FP

The TP and FP rates were plotted on the y-axis and x-axis of the ROC, respectively. The AUC value shows the model success rate by engaging the training dataset and its prediction rate by engaging the test dataset, using the ArcSDM ROC tool. The success rate describes how well the model fits with past landslide occurrences. On the other hand, prediction rate describes how well the model predicts occurrences of landslides in future (Pham *et al.,* 2015; Pradhan *et al.,* 2010). The AUC value ranges from 0.5 to 1(Nohani *et al., 2019*). The higher the value of the AUC, the better the performance of the model (Gudiyangada *et al., 2019*).

RESULTS

Landslide Inventory

A total of 47 landslide scars were identified, and then divided into two groups: - a) 35 landslides as the training dataset and b) 12 landslides for validation of the model (*Figure 1*). Considering land use, the largest proportion of landslides were identified in cultivated areas, while the least occurrences were identified in forested areas. Equal number of landslides were identified in bare lands, wood lands, and in built-up areas. Some of these landslides occurred very close to homes (*Figure 12).* Concerning lithology, most of the landslides occurred in areas with biotite granite, and each of the areas characterised with agglomerates and metagreywacke accounted for the least number of landslides in equal proportion. Most of the landslides were identified in the west and north aspects of slope. No landslide was identified in the flat slopes. Considering both profile and plan curvatures, the negative slopes bore the least landslide disasters. Similarly, very few (8.57%) landslides were identified in areas receiving less than 1650 mm/year of rainfall. More than half of the total landslides occurred in areas that receive 1650-1700 mm/year. More than 75% of the landslides were identified in areas with slopes of exceeding 10˚. Additionally, almost all the documented landslides were in cultivated areas. Built-up areas, woodlands, and bare lands had equally very low landslide numbers. Finally, the largest number of landslides were identified in areas with elevation above 1,997 m while only a few landslide disasters were occurred below 1497 m.

Article DOI: https://doi.org/10.37284/eajenr.5.1.600

Figure 12: A landslide very close to a home in Bundesi Parish. Photo taken by Mande, November 2020

Influence of the Conditioning Parameters on Landslide Occurrence

The results from the analysis using the weights of evidence for the selected conditioning parameters (*Figures 4 to 11*) are presented in *Table 2*. The negative values of the weights indicate that such class is not favourable to landslide occurrence, while a positive weight indicates that the presence of that class favours landslide disasters. The C/s(C), the ratio of the contrast to the standardised contrast, is the final weight, which is taken as the overall contribution of a factor class to landslide susceptibility.

Of all the parameter classes, cultivated areas had the largest positive weight (C/s(C) = 2.478), followed by slope angles which was greater than 40 (C/s(C) = 2.045), biotite granite lithology (C/s(C) = 1.697), elevation of 1397-1497 m (C/s(C) = 1.642) and north oriented slopes (C/s(C) = 1.490). This is an indication that slopes with a combination of these classes are highly predisposed to landslide occurrence. On the other hand, the largest negative standardised contrast values were seen in areas characterised with agglomerates (C/s(C) = -1.882), and elevations ranging between 1897 and 1997 m (C/s(C) = -1.263). Such large negative values demonstrates that these classes are not important in triggering landslides in the study area.

Article DOI: https://doi.org/10.37284/eajenr.5.1.600

Table 2: Weights of evidence analysis between the training dataset and conditioning factors

Factor		Area (%)	Landslides (%)	W+	S(W+)	W-	S(W-)	C	S (C)
Rain (mm/yr)	<1650	7.29	8.57	0.162	0.209	0.282	0.289	-0.402	0.357
	1650 – 1700	74.11	65.71	-0.120	0.578	-0.014	0.177	0.176	0.605
	>1700	18.60	25.71	0.325	0.334	-0.092	0.196	0.416	0.387
Slope angle (degrees)	<10	13.06	8.57	-0.392	0.578	0.048	0.180	-0.440	0.605
	10 - 30.	31.27	40.00	0.276	0.268	-0.156	0.224	0.432	0.349
	20 – 30	34.49	25.71	-0.265	0.334	0.116	0.200	-0.381	0.389
	30 – 40	18.46	17.14	-0.228	0.448	0.045	0.186	-0.273	0.485
	>40	2.74	8.57	1.176	0.579	-0.065	0.180	1.240	0.606
Elevation (m.a.s.l)	1397 – 1497	1.86	5.71	1.158	0.709	-0.042	0.177	1.200	0.731
	1497-1597	12.00	17.14	0.387	0.409	-0.067	0.189	0.453	0.451
	1597-1697	17.01	14.29	-0.146	0.448	0.028	0.186	-0.174	0.485
	1697-1797	29.06	31.43	0.107	0.302	-0.048	0.209	0.155	0.367
	1797-1897	22.21	17.14	-0.230	0.409	0.057	0.189	-0.288	0.450
	1897-1997	13.55	5.71	-0.836	0.707	0.085	0.177	-0.921	0.729
	1997-2097	4.01	5.71	0.385	0.708	-0.020	0.177	0.405	0.730
	>2097	0.30	2.86	-0.008	0.001	0.447	0.174	-0.009	0.480
Slope aspect	Flat	0.31	0.00	0.000	0.000	0.000	0.000	0.000	0.000
	North	32.12	28.57	0.383	-0.137	0.289	0.196	0.520	0.349
	East	6.54	11.43	0.300	0.578	-0.025	0.180	0.325	0.605
	South	26.91	25.71	-0.016	0.334	0.006	0.200	-0.022	0.389
	West	34.12	34.29	0.034	0.289	-0.018	0.213	0.052	0.359
Profile curvature	Negative	15.48	14.29	-0.051	0.448	0.009	0.186	-0.060	0.485
	Zero/flat	36.66	45.71	0.186	0.259	-0.126	0.230	0.311	0.346
	Positive	47.86	40.00	-0.151	0.268	0.121	0.224	-0.272	0.349
Plan curvature	Negative	20.73	17.14	-0.161	0.409	0.038	0.189	-0.200	0.450
	Zero/flat	33.69	34.29	-0.041	0.302	0.020	0.209	-0.060	0.367
	Positive	45.58	48.57	0.093	0.243	-0.085	0.243	0.178	0.343
Lithology	A3Tbg	82.76	94.29	0.131	0.174	-1.106	0.707	1.236	0.729
	A3WBgw	0.69	2.86	1.422	1.004	-0.022	0.172	1.444	1.019
	NeEag	16.54	2.86	-1.758	1.000	0.152	0.172	-1.910	1.015
Land use	Woodlands	4.10	5.71	0.332	0.708	-0.017	0.174	0.349	0.729
	Forested areas	2.46	2.86	-0.090	0.018	0.408	0.177	-0.107	0.445

Article DOI: https://doi.org/10.37284/eajenr.5.1.600

Factor		Area (%)	Landslides (%)	W+	S(W+)	W-	S(W-)	C	S (C)
	Cultivated areas	87.88	80.00	1.429	-0.063	0.578	0.169	1.493	0.602
	Built-up areas	1.47	5.71	1.366	0.710	-0.044	0.174	1.410	0.731
	Bare lands	4.09	5.71	0.335	0.708	-0.017	0.174	0.352	0.729

Article DOI: https://doi.org/10.37284/eajenr.5.1.600

Landslide Susceptibility

Analysis of the weights together with the training landslide points reveals that whereas the eastern and northern part of the study area is the least susceptible to landslide occurrence, the southwest areas are the most susceptible (*Figure 13).* The percentage of the area classified under each susceptibility category was as follows: 18.84% in the very low class, 24.81% in the low class, 333.85% in the moderate class, 19.77% in the high class, and 2.73% in very high susceptibility class. This shows that the largest part of the study area was predicted as having moderate susceptibility to landslides. Moreover, Bukibumbi, Bundesi, Nabulalo, and Suume parishes were identified as being more likely to experience landslide disasters in future. Shibanga Parish was considered to be relatively least prone to landslides disasters. It is also important to note that these classes are not absolute but rather relative degrees of susceptibility.

Figure 13: Landslide susceptibility map of the study area

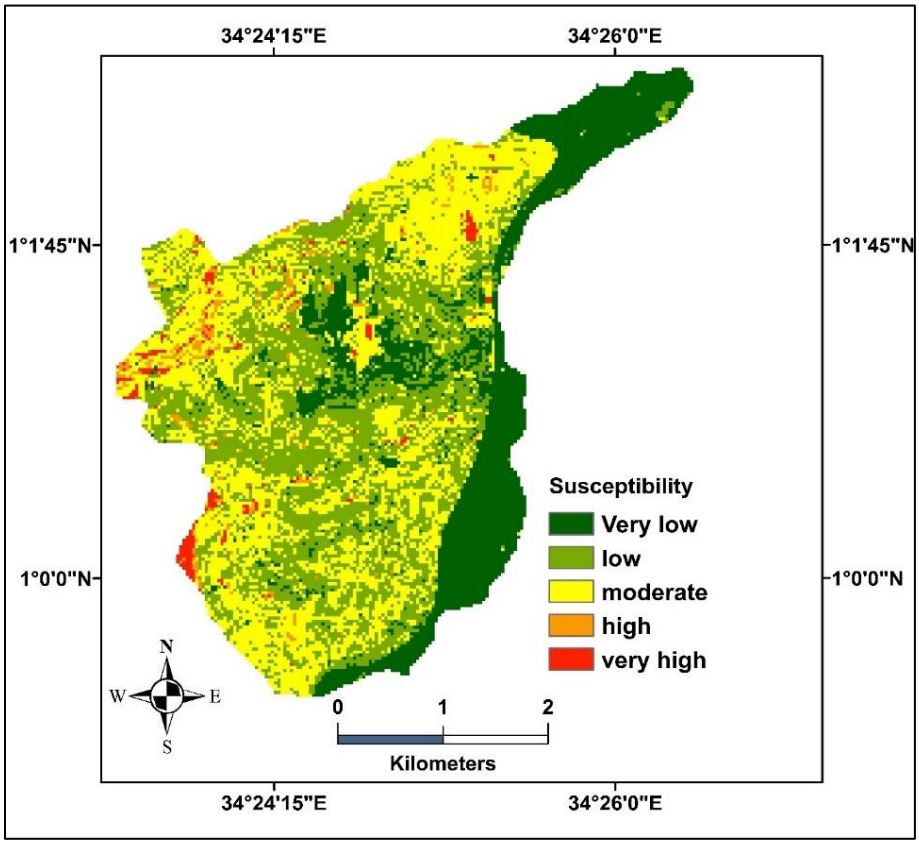

Conditional Independence

The probability that this model is not conditionally independent was 62.5%, which is an acceptable value given the rule that probability values greater than 95% indicate that the hypothesis of conditional independence should be rejected (Nohani *et al.*, 2019; Pham *et al.*, 2015; Pradhan *et al.*, 2010). Thus, the hypothesis of conditional independence among the eight landslide conditional factors is accepted. The test also revealed an overall CI accuracy of 85.0%, which indicates sufficient accuracy. Therefore, the results of the Agterberg–Cheng test demonstrate that the conditioning factors used in this study are suitable for predicting landslides.

Validation

Analysis using the training dataset generated a ROC with an AUC value equal to 0.882 (*Figure 14*), which is considered a reasonable value (Nohani *et al., 2019*). This demonstrates that the weights of

Article DOI: https://doi.org/10.37284/eajenr.5.1.600

evidence model fit well with past landslide disasters. Secondly, the ROC from the validation dataset yielded an AUC value of 0.912 (*Figure 15*), which is considered an indicator of very good prediction rate as demonstrated by other studies (Canavesi *et al., 2020*; Chen *et al., 2019*; Manchar *et al., 2018*). Therefore, the model and the considered conditioning factors performed reasonably well in predicting future landslides in the study area. Lastly, the ROC curves for both prediction rate and success rate are above the random guess line. This shows that the model performs with greater accuracy in landslide susceptibility, effectively better than by simple chance. Therefore, the resulting susceptibility map is adequately reliable, and could be used by decision makers, engineers, and government organizations to better planning for sustainable development (Elmoulat & Lahcen, 2018).

Figure 14: ROC curve to show the success rate of the model

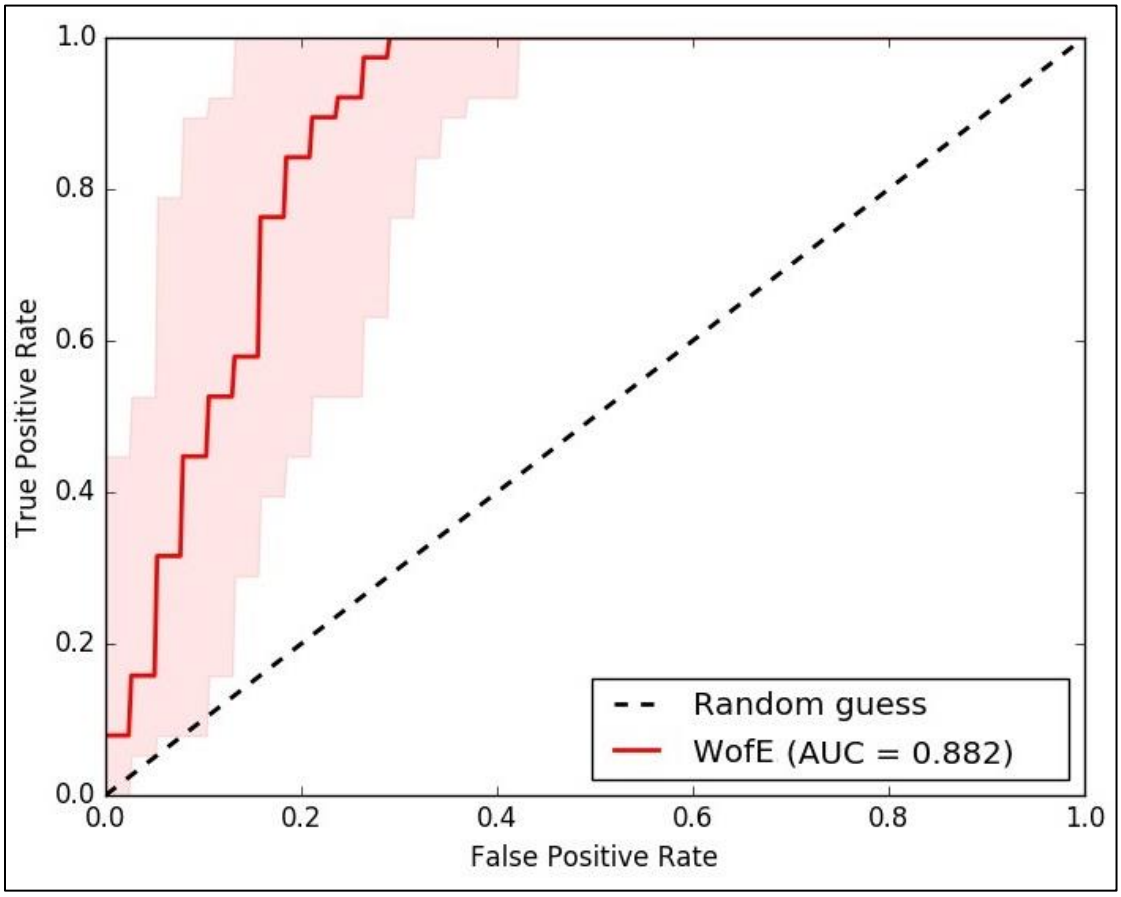

Article DOI: https://doi.org/10.37284/eajenr.5.1.600

Figure 15: ROC curve to show the prediction rate of the model

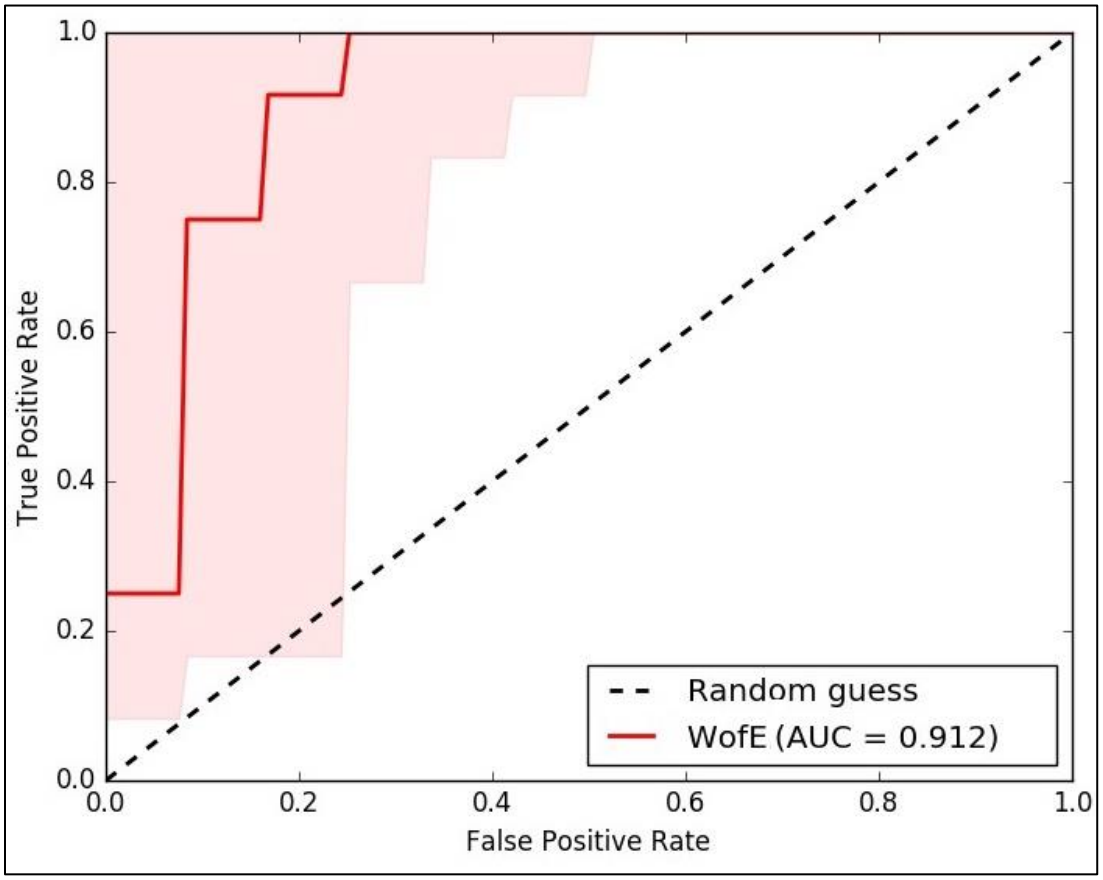

DISCUSSION

Influence of the Selected Conditioning Factors

Weight of evidence analysis revealed that the north-facing slopes are the most favourable to potential landslides, which could be attributed to its reception of least sunshine relative to other slopes (Nohani *et al., 2019*), hence moister. This finding is also in agreement with similar studies (Mugagga *et al., 2012*) that reported relatively more landslide processes in the north-oriented slopes. Slopes characterised by flat profile and positive plan curvature similarly had positive weights of influence on landslides, which when compounded with other factors predisposes a slope to landslides.

Of the three types of lithology identified in the watershed, biotite granite lithology had very high positive influence on landslide occurrence possibly because of forming soils with high clay content that are prone to slope failure (Kitutu, 2010). This also demonstrates the role of the inherent factors that determine the nature of the soils in the area.

Flat slopes did not show any significant importance in predicting landslides, because materials cannot slide on flat surfaces under the pull of gravity. The perpendicular force is highest on flat slopes (Chen *et al., 2019*), and, therefore, unlikely to slide. It was also noted that lower elevations (1397-1597 m) had higher influence to landslides which can be explained by the removal of forest cover (Mugagga *et al., 2012*). This collaborates the findings of (Nohani *et al., 2019*) that report lowest elevation as having greater impacts on landslides.

The high weights for the cultivated areas are expected because cultivation involves clearing existing vegetation, and tilling the ground. Such activities modify and cumulatively lower the threshold of slope stability, leading to its likely failure (Mugagga *et al., 2012*). Built-up areas are also associated with slope cutting for foundations. Building roofs additionally collect and redirect rain

Article DOI: https://doi.org/10.37284/eajenr.5.1.600

water in large volumes, increasing the water pressure as it flows downhill. This can potentially trigger landslides. On the contrary, forested areas are rich with vegetation whose roots further bind the soil materials and stabilise slopes (Kitutu *et al., 2009*; Nohani *et al., 2019*). This could explain their reported negative weights of influence on susceptibility to landslides in the area.

Rainfall has been reported as the major triggering factor to landslides on the slopes of Mount Elgon (Kitutu, 2010). Likewise, this study indicates that rainfall amounts greater than 1650 mm/year can potentially lead to landslide disasters. This is because rain water saturates the soil and increases the soil moisture content, in addition to acting as a lubricant of clay minerals which facilitates their sliding. This is further compounded by the concentration of rain in two wet seasons per year (Staudt *et al., 2014*). This study also demonstrated that landslides can occur in forested areas, despite having negative weights and thus negative correlation to landslides. This finding is in agreement with previous studies in the region that identified landslides in a forested area in Kitati, Sironko District attributed to soils with clay content well above 20% Mugagga et al (2012).

As suggested by the weights of evidence analysis in this study, slopes with higher gradients are more susceptible to landslides. As slope angle increases, the shear stress in the soil or other unconsolidated material generally increases and the landslide probability becomes higher (Chen *et al., 2019*). This study also demonstrated the high influence of lithology on the landslide occurrence in the area, as indicated by their high weights. By implication, inherent factors are very important in the overall stability of a slope, and can further be exacerbated by human interference.

Landslide Susceptibility

The final landslide susceptibility map (LSM) predicted a large part of the study area (52.70%) as having moderate and high susceptibility to landslides. By implication, the landslides are more likely to occur in the area under the present conditions. Furthermore, 37.03% and 34.94% of the study area classified as very highly susceptible to landslides lie in Bukibumbi and Bundesi parishes, respectively. Hence these two parishes are particularly noteworthy in their contribution to the overall high susceptibility of the study area. This equally points to the significance of potential landslide disasters in the study area. The relatively high susceptibility to landslides in Bukibumbi Parish can be explained by the relatively high population density in the area: 729 people per square kilometre, which forces people to concentrate their activities on steeper slopes (Chen & Li, 2014). The highest population in Bukalasi Sub County was also recorded in the same parish (1,962 people) according to the 2014 national census (Uganda Bureau of Statistics, 2018). Furthermore, much of Bukibumbi Parish is under the cultivated area land use type, which the weights of evidence analysis have indicated to strongly favour landslides. Other studies have likewise reported the strong influence of cultivation on slope failures (Xing *et al., 2021*).

CONCLUSION AND RECOMMENDATIONS

The area's natural characteristics, such as elevation, lithology, slope angle, slope aspect and slope curvature predispose the study area landslide. Generally, the relative importance of the conditioning factors considered in this study decreases in the order of; lithology>land use>slope aspect>rainfall>slope angle>elevation>curvature. Contrast values also show that landslide disasters are more likely in cultivated areas, and in areas characterised by biotite granite lithology. In regards to slope aspect, the north facing slopes are most prone to landslide occurrence. Further still, susceptibility to landslides generally increases with rainfall and slope angle. On the other hand, forests have strong negative correlation to landslides, and, therefore, such areas are relatively stable and less prone to landslide disasters.

Based on the landslide susceptibility map of the milli-watershed, intervention programs, such as government relocations plans should prioritise residents in the high susceptibility areas. These include especially those living on steep slopes, or those whose gardens are in those areas in order to minimise slope disturbance. Deforestation should have severe penalties since forests have been shown to reduce landslide susceptibility. Other human activities like farming on fragile slopes, that would

Article DOI: https://doi.org/10.37284/eajenr.5.1.600

further destabilise the slopes should also be discouraged. Instead, extensive reforestation programs should be implemented on slopes that have been indicated to be more susceptible to landslide processes, such as the north facing slopes, to reduce the likelihood of landslides in the area. Development activities such as infrastructural developments and settlements should be well planned to avoid the more unstable slopes that are indicated to favour landslides. This would reduce losses in the event of landslide occurrences. Although this study predicts the area's susceptibility to landslides, further studies are recommended to understand how each of the conditioning parameters contribute to landslides, and the synergetic interactions among these factors if any.

ACKNOWLEDGEMENTS

The authors wish to thank Mr. Martin Ekiryagana of DGSM Entebbe, Uganda and Mr. Samuel Ekwacu of UNMA, Uganda, for their help with some of the secondary data used in this study.

DECLARATION OF INTEREST STATEMENT

The authors declare that no conflict of interests exist.

REFERENCES

Agterberg, F. P., & Cheng, Q. (2002). Conditional independence test for weights-of-evidence modeling. *Natural Resources Research*, *11*(4), 249-255.

Benchelha, S., Aoudjehane, H. C., Hakdaoui, M., El Hamdouni, R., Mansouri, H., Benchelha, T., & Alaoui, M. (2019). Landslide susceptibility mapping in the Municipality of Oudka, Northern Morocco: a comparison between logistic regression and artificial neural networks models. *The International Archives of Photogrammetry, Remote Sensing and Spatial Information Sciences*, *42*, 41-49.

Broeckx, J., Maertens, M., Isabirye, M., Namazzi, B., Tamale, J., Jacobs, L., ... & Poesen, J. (2018, April). Landslide susceptibility and rates in the Mount Elgon region, Uganda. In *EGU General Assembly Conference Abstracts* (p. 16682).

Byou, T. (2021). Evaluation of the landslide susceptibility map obtained by a GIS matrix method: a case of Al Hoceima city (northern Morocco). In *SHS Web of Conferences* (Vol. 119). EDP Sciences.

Canavesi, V., Segoni, S., Rosi, A., Ting, X., Nery, T., Catani, F., & Casagli, N. (2020). Different approaches to use morphometric attributes in landslide susceptibility mapping based on meso-scale spatial units: A case study in Rio de Janeiro (Brazil). *Remote Sensing*, *12*(11), 1826.

Chen, W., & Li, W. (2014). Application of weights-of-evidence model in landslide susceptibility mapping at Baozhong Region in Baoji, China. *EJGE*, *19*.

Chen, W., Sun, Z., & Han, J. (2019). Landslide susceptibility modeling using integrated ensemble weights of evidence with logistic regression and random forest models. *Applied sciences*, *9*(1), 171.

Devkota, K. C., Regmi, A. D., Pourghasemi, H. R., Yoshida, K., Pradhan, B., Ryu, I. C., ... & Althuwaynee, O. F. (2013). Landslide susceptibility mapping using certainty factor, index of entropy and logistic regression models in GIS and their comparison at Mugling–Narayanghat road section in Nepal Himalaya. *Natural hazards*, *65*(1), 135-165.

Elmoulat, M., & Ait Brahim, L. (2018). Landslides susceptibility mapping using GIS and weights of evidence model in Tetouan-Ras-Mazari area (Northern Morocco). *Geomatics, Natural Hazards and Risk*, *9*(1), 1306-1325.

Froude, M. J., & Petley, D. N. (2018). Global fatal landslide occurrence from 2004 to 2016. *Natural Hazards and Earth System Sciences*, *18*(8), 2161-2181.

Gadtaula, A., & Dhakal, S. (2019). Landslide susceptibility mapping using weight of evidence method in Haku, Rasuwa district, Nepal. *Journal of Nepal Geological Society*, *58*, 163-171.

Gorokhovich, Y., Doocy, S., Walyawula, F., Muwanga, A., & Nardi, F. (2013). Landslides in Bududa, Eastern Uganda: Preliminary

Article DOI: https://doi.org/10.37284/eajenr.5.1.600

assessment and proposed solutions. In *Landslide science and practice* (pp. 145-149). Springer, Berlin, Heidelberg.

Gudiyangada Nachappa, T., Tavakkoli Piralilou, S., Ghorbanzadeh, O., Shahabi, H., & Blaschke, T. (2019). Landslide susceptibility mapping for Austria using geons and optimization with the Dempster-Shafer theory. *Applied Sciences*, *9*(24), 5393.

Guzzetti, F., Mondini, A. C., Cardinali, M., Fiorucci, F., Santangelo, M., & Chang, K. T. (2012). Landslide inventory maps: New tools for an old problem. *Earth-Science Reviews*, *112*(1-2), 42-66.

IPCC. (2014). Climate Change 2014: Synthesis Report. C*ontribution of Working Groups I, II, and III to the Fifth Assesment Report of the Intergovernemental Panel on Climate Change*. Geneva, Switzerland: IPCC. pp.http://www.ipcc.ch/report/ar5/syr//hdl:10013/epic.45156.d001

Kitutu, K. M. G. (2010). *Landslide occurrences in the hilly areas of Bududa District in Eastern Uganda and their causes* (Doctoral dissertation, Makerere University).

Kitutu, M. G., Muwanga, A., Poesen, J., & Deckers, J. A. (2009). Influence of soil properties on landslide occurrences in Bududa district, Eastern Uganda. *African journal of agricultural research*, *4*(7), 611-620.

Li, B., Wang, N., & Chen, J. (2021). GIS-based landslide susceptibility mapping using information, frequency ratio, and artificial neural network methods in Qinghai Province, Northwestern China. *Advances in Civil Engineering*, *2021*.

Manchar, N., Benabbas, C., Hadji, R., Bouaicha, F., & Grecu, F. (2018). Landslide susceptibility assessment in Constantine region (NE Algeria) by means of statistical models. *Studia Geotechnica et Mechanica*, *40*(3), 208-219.

Maxwell, A. E., Warner, T. A., & Guillén, L. A. (2021). Accuracy assessment in convolutional neural network-based deep learning remote sensing studies—part 1: Literature review. *Remote Sensing*, *13*(13), 2450.

Mugagga, F., Kakembo, V., & Buyinza, M. (2012). Land use changes on the slopes of Mount Elgon and the implications for the occurrence of landslides. *Catena*, *90*, 39-46.

Mugagga, F., Kakembo, V., & Buyinza, M. (2011). A characterisation of the physical properties of soil and the implications for landslide occurrence on the slopes of Mount Elgon, Eastern Uganda. *Natural hazards*, *60*(3), 1113-1131.

Nakileza, B. R., & Nedala, S. (2020). Topographic influence on landslides characteristics and implication for risk management in upper Manafwa catchment, Mt Elgon Uganda. *Geoenvironmental Disasters*, *7*(1), 1-13.

National Planning Authority (2020*). Third National Development Plan (NDPIII) 2020/21 – 2024/25*. National Planning Authority. http://www.npa.go.ug/wp-content/uploads/2020/08/NDPIII-Finale_Compressed.pdf.

Neema, S., Bua, G. M., Tuhebwe, D., Ssentongo, J., Tumuhamye, N., Mayega, R. W., ... & Bazeyo, W. (2018). Community perspective on policy options for resettlement management: A case study of risk reduction in Bududa, eastern Uganda. *PLoS currents*, *10*.

Nohani, E., Moharrami, M., Sharafi, S., Khosravi, K., Pradhan, B., Pham, B. T., ... & M Melesse, A. (2019). Landslide susceptibility mapping using different GIS-based bivariate models. *Water*, *11*(7), 1402.

Pham, B. T., Tien Bui, D., Indra, P., & Dholakia, M. (2015). Landslide susceptibility assessment at a part of Uttarakhand Himalaya, India using GIS–based statistical approach of frequency ratio method. *Int J Eng Res Technol*, *4*(11), 338-344.

Pradhan, B., Oh, H. J., & Buchroithner, M. (2010). Weights-of-evidence model applied to landslide susceptibility mapping in a tropical hilly area. *Geomatics, Natural Hazards and Risk*, *1*(3), 199-223.

Article DOI: https://doi.org/10.37284/eajenr.5.1.600

Staudt, M., Kuosmanen, E., Babirye, P., & Lugaizi, I. (2014). The Bududa landslide of 1 March 2010. *Geological Survey of Finland (Special Paper 56), 373*, *384*.

Uganda Bureau of Statistics. (2018*). Population by Parish Census 2014 Eastern Region, Kampala, Uganda*. Uganda Bureau of Statistics.

Vakhshoori, V., & Zare, M. (2018). Is the ROC curve a reliable tool to compare the validity of landslide susceptibility maps?. *Geomatics, Natural Hazards and Risk*, *9*(1), 249-266.

Van Den Eeckhaut, M., Hervás, J., Jaedicke, C., Malet, J. P., Montanarella, L., & Nadim, F. (2012). Statistical modelling of Europe-wide landslide susceptibility using limited landslide inventory data. *Landslides*, *9*(3), 357-369.

Xing, Y., Yue, J., Guo, Z., Chen, Y., Hu, J., & Travé, A. (2021). Large-scale landslide susceptibility mapping using an integrated machine learning model: A case study in the Lvliang mountains of China. *Frontiers in Earth Science*, 622.

Yalcin, A., Reis, S., Aydinoglu, A. C., & Yomralioglu, T. (2011). A GIS-based comparative study of frequency ratio, analytical hierarchy process, bivariate statistics and logistics regression methods for landslide susceptibility mapping in Trabzon, NE Turkey. *Catena*, *85*(3), 274-287.

